

1 SUPPLEMENTARY INFORMATION

2
3 **HSP70-mediated mitochondrial dynamics and autophagy represent a novel vulnerability in**
4 **pancreatic cancer**

5
6 Giulia D. S. Ferretti^{1,2,9}, Colleen E. Quaas^{1,2,9}, Irene Bertolini³, Alessandro Zuccotti^{1,2}, Ozge
7 Saatci^{1,2}, Jennifer A. Kashatus⁴, Salma Sharmin⁴, David Y. Lu³, Adi Narayana Reddy Poli³, Abigail
8 F. Quesnelle^{1,2}, Jezabel Rodriguez-Blanco^{2,5}, Aguirre A. de Cubas^{2,6}, G. Aaron Hobbs^{2,7}, Qin Liu³,
9 John P. O'Bryan^{2,7,8}, Joseph M. Salvino³, David F. Kashatus⁴, Ozgur Sahin^{1,2} and Thibaut
10 Barnoud^{1,2*}

11
12 ¹Department of Biochemistry and Molecular Biology, Medical University of South Carolina,
13 Charleston SC; ²Hollings Cancer Center, Medical University of South Carolina, Charleston SC;
14 ³Molecular and Cellular Oncogenesis Program, The Wistar Institute, Philadelphia PA; ⁴Department
15 of Microbiology, Immunology, and Cancer Biology, University of Virginia Health System,
16 Charlottesville VA; ⁵Darby Children's Research Institute, Department of Pediatrics, Medical
17 University of South Carolina, Charleston SC; ⁶Department of Microbiology and Immunology,
18 Medical University of South Carolina, Charleston SC; ⁷Department of Cell and Molecular
19 Pharmacology and Experimental Therapeutics, Medical University of South Carolina, Charleston
20 SC; ⁸Ralph H. Johnson VA Medical Center, Charleston SC.

21
22 **Running Title:** HSP70 regulates mitochondrial dynamics and autophagy

23
24 ⁹G.D.S.F. and C.E.Q. contributed equally to this manuscript

25
26 **Corresponding Author:**

27 Thibaut Barnoud, PhD
28 Assistant Professor
29 Department of Biochemistry & Molecular Biology
30 Medical University of South Carolina, Hollings Cancer Center
31 86 Johnathan Lucas St, HO512E
32 Charleston, SC 29425
33 Phone: (843) 792-3535
34 Email: barnoud@musc.edu

35 **Supplementary Materials and Methods**

36

37 **Antibodies and Reagents**

38 Antibodies used were purchased from: GAPDH (2118S), Cleaved Caspase 3 (9661S), Cleaved
39 Lamin A (2035S), HSP70 (4873S), ERK (4695T), AKT (9272S), GSK-3 β (12456T), CDK5
40 (2506S), CDK1/cdc2 (9116T), Phospho-Beclin 1 (S93; 14717S), Beclin 1 (4122S), BAK
41 (12105S), LC3B (3868T), PARP (9542S), Snail (3879T), Slug (9585T), β -Catenin (8480T), Ki-67
42 (9449S), CD31 (77699S), PINK1 (6946T), Phospho-DRP1 (S616; 4494S), and DRP1 (14647S),
43 Phospho-DRP1 (S637; 6319S), β -Actin (5125S), phospho-AMPK α (2535T), AMPK α (5832T),
44 phospho-ERK (4370T), and ERK (4695S) (Cell Signaling Technology, Danvers, MA, USA);
45 MRPS14 (ab151118) (Abcam, Cambridge, MA, USA); PINK1 (23274-1-AP) (Proteintech,
46 Rosemont, IL, USA); HSP70 (C92F3A-5) (Enzo Life Sciences, Farmingdale, NY, USA); HSC70
47 (sc-7298), GRP75 (sc-133137), and PINK1 (SC-518052) (Santa Cruz Biotechnology, Dallas, TX,
48 USA); and NDUFA6 (GTX65550) (GeneTex, Irvine, CA, USA). The following fluorescent
49 secondary antibodies were purchased from Thermo Fisher Scientific: Donkey anti-Mouse Alexa
50 Fluor 488 (A-21202), Goat anti-Rabbit Alexa Fluor 647 (A-21244), Goat anti-Rabbit Alexa Fluor
51 488 (A-21206), and Goat anti-Rat Alexa Fluor 594 (A-48264). Mouse (7076S), rabbit (7074S),
52 rat (7077S), and rabbit light-chain specific (93702S) secondary antibodies were purchased from
53 Cell Signaling Technology. AP-4-139B was generously provided by Dr. Maureen Murphy (The
54 Wistar Institute, Philadelphia, PA, USA). VER-155008 (HY-10941), 17-AAG (HY-10211), and
55 Hydroxychloroquine (HY-B1370) were purchased from MedChemExpress (Monmouth Junction,
56 NJ, USA). Spautin-1 (Item No. 17769) and MRT68921 (Item No. 19905) were purchased from
57 Cayman Chemical (Ann Arbor, MI, USA). Chloroquine diphosphate salt (CQ; C6628) and Mito-
58 TEMPO (SML0737-5MG) were purchased from MilliporeSigma (St. Louis, MO, USA).

59 Cycloheximide (CHX; J66901-03) was purchased from Thermo Fisher Scientific (Waltham, MA,
60 USA). For *in vitro* studies, AP-4-139B, PET-16, and VER-155008 were dissolved in DMSO. CQ,
61 CHX, and Mito-TEMPO were dissolved in molecular grade water.

62

63 **Generation of HSP70 gene knockout cell lines**

64 HSP70 knockout (KO) MIA PaCa-2 cells were generated by the Genome Engineering & Stem Cell
65 Center (GESCC@MGI) at the Washington University in Saint Louis. The guide RNA (gRNA)
66 sequence for KO of *HSPA1A/1B* is ‘atggccaaagccgcgcgcat’ followed by an NGG PAM site. A
67 random guide sequence targeting no known human genes was used as a control. Briefly, knockout
68 pools were nucleofected using a Lonza 4D nucleofection system (150,000 cells per 20 μ L reaction)
69 in P3 solution with program EH-100, with 1 μ L WT spCas9 protein (Macrolabs) and 1 μ L 100 μ M
70 sgRNA (obtained from Integrated DNA Technologies), recovered for 72 hours in 500 μ L growth
71 medium, then harvested for next generation sequencing (NGS) genotyping (Illumina sequencing)
72 and expansion of pools. Clonal isolation of pools was performed using a Sony SH-800 cell sorter,
73 genotypes were confirmed by NGS, and cell identify was confirmed by short tandem repeat (STR)
74 profiling. All clones were confirmed as negative for mycoplasma contamination prior to
75 cryopreservation.

76

77 **Western blot analysis and Immunohistochemistry (IHC)**

78 Western blot analyses and IHC were performed as described¹⁻⁴. Briefly, 3×10^5 - 7.5×10^5 cells were
79 plated in 10cm tissue culture plates (10861-680; VWR International, Radnor, PA, USA) and treated
80 as described. Cells were then harvested after the indicated timepoints and lysed with 1X RIPA
81 buffer (89901; Thermo Fisher Scientific) supplemented with protease and phosphatase inhibitors

82 (11836170001 and 4906845001; purchased from MilliporeSigma). 25-100 μ g of protein was run
83 over SDS-PAGE gels using 10% NuPAGE Bis-Tris pre-cast gels (NP0301; Thermo Fisher
84 Scientific) and were transferred onto polyvinylidene difluoride (PVDF) membranes (IPVH0010,
85 pore size: 0.45 μ m; MilliporeSigma). 15% SDS-polyacrylamide gels were used to obtain efficient
86 separation and detection of LC3-I and LC3-II bands by Western blot. Following transfer,
87 membranes were blocked using either 5% nonfat dry milk or 5% BSA (9999 or 9998, respectively;
88 Cell Signaling Technology) for one hour at room temperature. Membranes were probed with
89 indicated antibodies at 4°C overnight. Rabbit or mouse secondary antibodies conjugated to
90 horseradish peroxidase (Cell Signaling Technology) were used at 1:5,000-1:20,000 dilutions and
91 treated with Pierce ECL Western blotting substrate (Thermo Fisher Scientific) for two minutes.
92 Protein levels were detected using autoradiography or the iBright CL1500 Imaging System
93 (Thermo Fisher Scientific). Densitometry analysis of proteins was conducted using ImageJ
94 software (NIH, Rockville, MD, USA). Paraffin embedding, tissue sectioning, and all IHC staining
95 was performed by the Histology and Immunohistochemistry Laboratory Core at the Medical
96 University of South Carolina. Images for IHC analysis were captured using a Leica DM2000 LED
97 microscope, and the number of positive cells were quantified by ImageJ.

98

99 **Cell viability, colony formation, and synergy assays**

100 Alamar Blue assays were performed as previously described^{5,6}. For Trypan Blue cell viability
101 assays, 5×10^5 PDAC cells were plated in 10 cm dishes. The next day, cells were treated with 10
102 μ M of the indicated compounds for 48 hours. Cells were then collected and resuspended in a 1:1
103 ratio of 1X PBS and Trypan Blue (15259-061; Thermo Fisher Scientific). Live cell count and total
104 cell count were determined manually using a hemocytometer. For colony formation assays, PK-8

105 and MIA PaCa-2 cells were seeded in 60 mm dishes (500 cells/dish) with the indicated
106 concentrations of each compound, or the combination of both inhibitors. After 7 (Mia PaCa-2) and
107 14 days (PK-8), cells were fixed with 4% formaldehyde, stained with crystal violet solution (0.1%
108 crystal violet in 10% ethanol), and washed abundantly with distilled water. Colony numbers were
109 determined by manually counting using ImageJ cell counter plugin. Drug synergy assays were
110 performed as previously described⁷. Briefly, 2000 cells/well of four PDAC cell lines (TCC-Pan2,
111 PK-8, MIA PaCa-2, and PANC-1) were plated in 96-well plates. The next day, cells were treated
112 with AP-4-139B in combination with one of three autophagy inhibitors (CQ, Spautin-1, or
113 MRT68921) at the indicated concentrations for 72 hours. Total live cell count was quantified via
114 Calcein staining (C3100MP; Thermo Fisher Scientific) and counted using a Celigo image
115 cytometer. The average of 10 negative control wells (DMSO) was compared to a Day 0 control
116 plate to determine base-line cell viability. Expected effect sizes for each treatment combination
117 were calculated according to the BLISS algorithm⁸. Expected effect size was divided by observed
118 effect size, and the results were then correlated to the corresponding heat maps where values >1
119 indicate antagonism (blue), =1 indicate additive (white), and <1 indicate synergy (red). All heat
120 maps were generated using GraphPad Prism software; representative heatmaps shown were
121 generated using average BLISS scores of two independent 96-well plates per experiment.

122

123 **Immunofluorescence (IF)**

124 For *in vitro* IF, PDAC cells were allowed to adhere overnight coverslips and subsequently fixed
125 for 15 minutes (1% paraformaldehyde + 2% sucrose in 1X PBS), permeabilized (10 minutes in 1X
126 PBS + 0.5% Triton X-100) and blocked for 30 minutes in the following solution: 1X PBS + 3%
127 BSA + 0.2% Triton X-100. Cells were then incubated with primary antibodies PINK1 (Santa Cruz;

128 1:50) and HSP70 (Cell Signaling Technology; 1:100) for one hour (37°C) and overnight (4°C).
129 Cells were then washed and incubated with the respective secondary antibodies (1:1,000). Nuclei
130 were stained with DAPI (1 µg/mL) for 10 minutes in 1X PBS. After washing with PBS, coverslips
131 were mounted with ProLong™ Diamond Antifade mounting medium (P36970; Thermo Fisher
132 Scientific) and images were acquired on a Zeiss LSM 880 NLO microscope using a 63X oil
133 objective with a 3.5X zoom. 3D images were generated using Imaris image analysis software. For
134 *in vivo* IF, tumor tissues were fixed in 10% (V/V) formalin, embedded in paraffin, and sectioned
135 by the Histology and Immunohistochemistry Core at the Medical University of South Carolina.
136 Paraffin-embedded tissues were deparaffinized in 100% xylene and rehydrated in decreasing
137 concentrations of ethanol. To eliminate fixation-caused autofluorescence, tissue sections were
138 incubated in 10 mM Sodium Citrate (pH 6.0) in a water bath (95°C) and cooled. Tissues were then
139 permeabilized (30 minutes) and blocked for 2 hours with the same buffers described above, then
140 incubated overnight with anti-PINK1 primary antibody (Proteintech – 1:400). Tissues were
141 washed three times with 1X PBS and then incubated with Alexa Fluor™ 488 (1:500) secondary
142 antibody. Slides were then washed 3 times, and nuclei were stained with DAPI (1 µg/mL) for 10
143 minutes in PBS and washed with distilled water to avoid PBS crystals. Coverslips were mounted
144 and tissues imaged as described above for *in vitro* IF. The same parameters were used for acquiring
145 all the images. Fluorescence intensity was measured using ImageJ Fiji software.

146

147 **Co-immunoprecipitation (co-IP) and Proximity Ligation Assays (PLA)**

148 PANC-1 and MIA PaCa-2 cells PDAC cells were allowed to adhere overnight. The next day, cells
149 were harvested and centrifuged for 5 minutes at 4°C and washed with 1X PBS. Cell pellets were
150 lysed in 300 µL of Pierce IP Lysis Buffer (87787; Thermo Fisher Scientific) with 1X Halt Protease

151 Phosphatase Inhibitor Cocktail (78440; Thermo Fisher Scientific) and incubated on ice for five
152 minutes. Lysates were spun at $13,000 \times g$ for ten minutes at 4°C . Protein extracts (4 mg) were
153 incubated with either 10 μg of either PINK1 antibody (Cell Signaling Technology) or with Rabbit
154 IgG (12-370; MilliporeSigma) for 1 hour at 4°C . HSP70 immunocomplexes were captured using
155 Protein A magnetic beads (10-001-D; Thermo Fisher Scientific) and rotated overnight at 4°C .
156 Beads were washed twice with lysis buffer, and 40 μL of $2\times$ Laemmli Sample Buffer were added
157 to the beads, and samples were boiled for 10 minutes at 95°C . PINK1/HSP70 association was
158 analyzed by Western blot as described above. For PLA, PANC-1 cells were grown on Lab-Tek II
159 8-well chamber slides and fixed with 4% paraformaldehyde (15710; Electron Microscopy
160 Sciences) followed by permeabilization with 0.25% Triton X-100 in 1X PBS (1132481001;
161 MilliporeSigma). Protein–protein interactions were assessed using the PLA Duolink In Situ Starter
162 Kit (DUO92101) (MilliporeSigma) according to the manufacturer's protocol, using the following
163 primary antibodies: PINK1 (Proteintech; 1:400) and HSP70 (Enzo; 1:50). Nuclei were stained
164 with DAPI (1 $\mu\text{g}/\text{mL}$) and the slides were mounted with ProLong™ Diamond Antifade mounting
165 medium and images were captured on a Zeiss LSM 880 NLO microscope using a 63X oil
166 objective. ImageJ Fiji software was used to quantify proximity ligation analyses (PLA) signals
167 using the ImageJ cell counter plugin.

168

169 **Plasmids, siRNA, transfections, and autophagic flux assays**

170 PINK1-YFP (101874), mScarlet-HSP70 (163790), and mScarlet-Vector (85042) plasmids were
171 purchased from Addgene (Watertown, MA, USA). For transient transfections, 1×10^6 PANC-1 cells
172 were plated in 10 cm dishes. The next day, 5 μg of each of the indicated plasmids were transfected
173 into cells using FuGENE 6 purchased from Promega (E2691; Madison, WI, USA) according to

174 the manufacturer's instructions. 48 hours later, PANC-1 cells were treated with 80µg/mL of
175 cycloheximide (CHX) and harvested at the indicated timepoints for Western Blot analysis. For
176 siRNA studies, Dharmacon™ scrambled control siRNA (D-001810-10-20), human *HSPA1A*
177 siRNA (L-005168-00-0010), and human *PRKAA1* siRNA (L-005027-00-0010) were purchased
178 from Revvity (Waltham, MA, USA). For siRNA transfections, 3x10⁵ PDAC cells were plated in
179 10-cm plates. siRNAs were transfected using Lipofectamine™ RNAiMAX transfection reagent
180 (13778-075; Thermo Fisher Scientific) in OPTI-MEM™ media (31985-070; Thermo Fisher
181 Scientific) according to the manufacturer's protocol. Cells were harvested 48 hours later for
182 Western blot analysis. Autophagic flux assays were performed as previously described⁹. Briefly,
183 PDAC cell lines were transduced with a pBABE-puro retroviral plasmid containing a mCherry-
184 EGFP-LC3B construct (22418; Addgene, Watertown, MA, USA). 1x10⁵ PDAC cells per quadrant
185 were plated on glass-bottomed plates (627870; Greiner Bio-One, Monroe, NC, USA) and treated
186 with vehicle or AP-4-139B for six hours at indicated concentrations. For concurrent treatment
187 with chloroquine (CQ), cells were pre-treated with CQ at the indicated concentrations overnight,
188 followed by treatment with AP-4-139B the next day for six hours. Cells were imaged using a Zeiss
189 510 LSM confocal microscope. To determine levels of autophagic flux, the ratio of total area
190 fluorescence of mCherry positive punctae and EGFP positive punctae was analyzed by ImageJ
191 software as described previously¹⁰.

192

193 **Mitochondrial oxygen consumption rates (OCR), Mito-TEMPO, and mitochondrial** 194 **depolarization assays**

195 Mitochondrial Oxygen Consumption Rates using the XF Mito Stress Test was performed as
196 previously described^{11,12}. 2x10⁴ PANC-1 and HPNE-DT cells, and 5x10⁴ MIA PaCa-2 cells, were
197 plated in Seahorse 96-well cell culture microplates, treated with AP-4-139B for 24 hours, and

218 subjected to the Seahorse XF Cell Mito Stress Test (103015-100), according to the manufacturer's
219 protocol (Agilent Technologies, Santa Clara, CA, USA). Briefly, cell medium was replaced with
220 Seahorse XF Base Medium (supplemented with 100 mM Pyruvate, 200 mM Glutamine, and 2.5
221 M Glucose) and incubated in a 37°C non-CO₂ incubator for one hour before the start of the assay.
222 Basal OCR was measured using the Seahorse XFe Extracellular Flux analyzer. Measurements
223 were performed after injection of three compounds affecting bioenergetics: 1 μM oligomycin, 1
224 μM carbonyl cyanide 4-(trifluoromethoxy) phenylhydrazone (FCCP), and 1 μM
225 Rotenone/Antimycin A; all inhibitors were purchased from Seahorse Bioscience. Data are
226 representative of three biological replicates. For experiments performed in the presence or absence
227 of Mito-TEMPO, PDAC cells were pre-treated for three hours with 10 μM Mito-TEMPO, and
228 subsequently treated with 5 μM AP-4-139B for another 24 hours. Cells were then harvested and
229 processed for Western Blot analysis. For mitochondrial membrane depolarization assays, PANC-
230 1 or MIA PaCa-2 cells were plated (2000 cells/well) in a 96-well plate and treated the following
231 day with the indicated doses of AP-4-139B for 24 hours. Cells were incubated with 50 nM TMRE
232 (T-669; Thermo Fisher Scientific) for 30 minutes at 37°C, followed by washing twice with 100 μL
233 of 1X PBS. A final volume of 100 μL of PBS was added to each well, and the fluorescence was
234 measured with the following excitation/emission: 544/590 nm. For TMRE measurements via
235 microscopy, 1x10⁵ PDAC cells were plated per quadrant on glass-bottomed plates (627870;
236 Greiner Bio-One) and treated with the indicated doses of AP-4-139B for 24 hours. Cells were then
237 stained with TMRE for 20 minutes at 37°C, washed twice with 1X PBS, and nuclei were stained
238 with two drops of Hoechst 33342 purchased from Thermo Fisher Scientific (R37605) and
239 immediately imaged on a Zeiss LSM 880 NLO microscope using a 63X oil objective. ImageJ Fiji
240 software was used to quantify the Intensity of TMRE fluorescence.

221 **Cortical mitochondrial analysis, time-lapse video-microscopy, and ROS production**

222 For cortical mitochondrial analysis, 1×10^4 MIA PaCa-2 and PANC-1 cells were seeded on
223 coverslips and treated with AP-4-139B (500nM and $1 \mu\text{M}$, respectively) for 24 hours. Cells were
224 stained with 100 nM MitoTracker deep red FM dye for 30 minutes at 37°C , washed, and fixed
225 with 4% formaldehyde for ten minutes. Actin filaments were stained with phalloidin 488 (Thermo
226 Fisher Scientific) for one hour, and nuclei were stained with Hoechst (Thermo Fisher Scientific)
227 for five minutes. Slides were analyzed on a Leica TCS SP5 confocal laser microscope with a 63X
228 oil objective and images were analyzed in ImageJ as described¹³. For time-lapse video-
229 microscopy, 1×10^4 MIA PaCa-2 and PANC-1 cells were seeded on high-optical-quality glass-
230 bottom 35-mm plates (MatTek Corporation) for 24 hours and then treated with 500nM or $1 \mu\text{M}$ of
231 AP-4-139B, respectively. Cells were then stained with MitoTracker Deep Red for 30 minutes at
232 37°C . Cells were imaged on a Leica TCS SP8 X inverted confocal laser scanning microscope
233 using a 63X, 1.40-numerical-aperture (NA) oil objective, and live imaging time-lapse video-
234 microscopy was performed using a Tokai Hit incubation chamber equilibrated to bidirectional
235 scanning at 8,000 Hz at 37°C with 5% CO_2 . Images were acquired every 3 seconds for a 1-minute
236 interval. Individual 12-bit images were acquired using a white-light supercontinuum laser (0.2%
237 at 643 nm) and hybrid detectors at a 4X digital zoom with a pixel size of 70 nm by 70 nm and a
238 step size of 0.260 μm . A minimum of six single cells under each condition were collected for
239 analysis. Initial postprocessing of 3D sequences was carried out as described¹⁴. Images were then
240 imported into Leica LAS X software to either measure mitochondrial motility or mitochondrial
241 fission and fusion events as described¹⁴. To detect intracellular ROS, MIA PaCa-2 and PANC-1
242 cells were treated with the indicated doses of AP-4-139B for 48 hours and then incubated with
243 either CellROX-Green (C10444; Thermo Fisher Scientific) or MitoSOX-Red (M36008; Thermo

244 Fisher Scientific), according to the manufacturer's instructions. Cells were harvested and analyzed
245 on a BD Biosciences FACSCelesta flow cytometer and intact cells were gated in the FSC/SSC plot
246 to exclude small debris. The resulting data were plotted on a histogram. For analysis of
247 mitochondrial morphology, 1,000 PANC-1 and MIA PaCa-2 cells were seeded on glass coverslips
248 and treated with AP-4-139B (2 μ M) for 24 hours. Cells were then treated with 50 nM MitoTracker
249 Red CMXRos (Thermo Fisher Scientific) for 30 minutes, fixed, permeabilized, and mounted
250 immediately using Prolong Gold antifade reagent with DAPI (P36935; Thermo Fisher Scientific).
251 Cells were imaged on a Zeiss LSM 900 Airyscan2 microscope using a 63X oil objective, and
252 mitochondrial morphologies were 3D surfaced mapped using Imaris microscopy image analysis
253 software.

254

255 **Tumor cell migration, motility and 2D chemotaxis**

256 Scratch assays were performed as previously described¹⁵. Briefly, MIA PaCa-2 and PANC-1 cells
257 were each seeded in 6-well plates and grown to form a confluent monolayer. Subsequently, two
258 linear scratches, oriented perpendicular to each other, were made in each well with sterile 200 μ L
259 pipette tips, and wells were then washed twice with PBS. DMSO was used as an untreated control,
260 and media with AP-4-139B at the indicated concentrations were added to the respective wells
261 before beginning time-lapse imaging with a Nikon Te300 Inverted Microscope (3 images/well, 2
262 wells/condition). Images were captured every four hours for 36 hours. Cell migration was
263 evaluated at 24- and 36-hour timepoints using ImageJ software (National Institutes of Health,
264 USA) and normalized to wounds at the 0-hour timepoint. Results are expressed as the percent
265 wound closure for each condition. For 2D motility studies, MIA PaCa-2 and PANC-1 cells (1×10^4)
266 were seeded in 4-well Ph+ chambers (80446; Ibidi USA, Inc., Fitchburg, WI, USA) in complete

267 medium. Cells were treated with the indicated doses of AP-4-139B for 24 hours. Time-lapse
268 video-microscopy was then performed over a 10-hour interval as described.¹⁶ Stacks were
269 imported into ImageJ Fiji software for analysis, and 30 cells per each condition tested were tracked
270 using the Manual Tracking plugin for ImageJ Fiji in 3 independent experiments. Tracking data
271 were exported into Chemotaxis and Migration Tool v. 2.0 (Ibidi USA, Inc.) for graphing and
272 calculation of means of speed and accumulated distance of movement.

273

274 **HSP70 Gene Expression Analysis**

275 The comparison of HSPA1A mRNA expression in normal, tumor, and metastatic site was
276 performed as previously described¹⁷⁻¹⁹. Briefly, the mRNA expression of *HSPA1A* in TCGA
277 tumors and matched normal tissue and in normal tissue from GTEx Biobank was retrieved using
278 the Xena Browser²⁰, USCS Santa Cruz (<https://xenabrowser.net/>). The data were represented as
279 scatter plots with mean and standard deviation using GraphPad Prism. The significance between
280 tumor vs. normal expression of *HSPA1A* was calculated by unpaired students' t-test. The three
281 cancer types where *HSPA1A* expression is significantly higher in tumors compared to normal
282 ($P<0.001$) were ordered with respect to the difference between tumor and normal means from
283 highest to lowest (i.e., PAAD, BRCA and SKCM). All the other cancer types were alphabetically
284 ordered. To compare *HSPA1A* mRNA expression between primary pancreatic tumors and
285 metastatic site, data from GSE71729 dataset²¹ were retrieved from the GEO depository
286 (<https://www.ncbi.nlm.nih.gov/geo/>) and represented as a scatter plot with mean and standard
287 deviation using GraphPad Prism. The significance was calculated by unpaired students' t-test. For
288 association of HSP70 expression and tumor grade, PAAD (pancreatic adenocarcinoma) patient
289 data from TCGA were stratified into three groups: Grade I, II, and III. Data are represented as

290 boxplots using the median expression for *HSPA1A* across three grades. Significance between
291 groups was determined using ANOVA with post hoc Tukey pairwise comparison. Boxplots were
292 generated using ggplot R package, and analysis was completed using RStudio software.

293

294 **Animal Studies**

295 For human xenograft studies, 2.5×10^6 PANC-1 or MIA PaCa-2 cells were injected subcutaneously
296 into the right flanks of 6–8-week-old female NSG (NOD.Cg-*Prkdc*^{scid} *Il2rg*^{tm1Wjl}/SzJ) mice; all
297 mice were purchased from the Jackson Laboratory. For PK-8 xenograft studies, 5×10^6 cells were
298 injected per mouse. Tumor volumes were measured using digital calipers and calculated using the
299 formula: volume = (length x width²) x 0.52. AP-4-139B was made as a stock solution of 100
300 mg/mL in DMSO and diluted to 2 mg/mL in 0.9% saline solution (S8776; MilliporeSigma), and
301 Hydroxychloroquine (HCQ) was made as a 2mg/mL stock in PBS. Mice were given either vehicle
302 control or 10mg/kg AP-4-139B every other day by intraperitoneal (i.p.) injection. For synergy
303 studies, HCQ was given at 50mg/kg every day by i.p. injection. For *in vivo* metastasis assays, 8–
304 10-week-old NSG mice were injected with 5×10^5 MIA PaCa-2 cells. Mice were then treated with
305 either vehicle or 10 mg/kg AP-4-139B by i.p. injection every 48 hours. There was no blinding
306 during *in vivo* experiments. Sample sizes were based on previous studies ²².

307

308

309

310

311

312

313

314

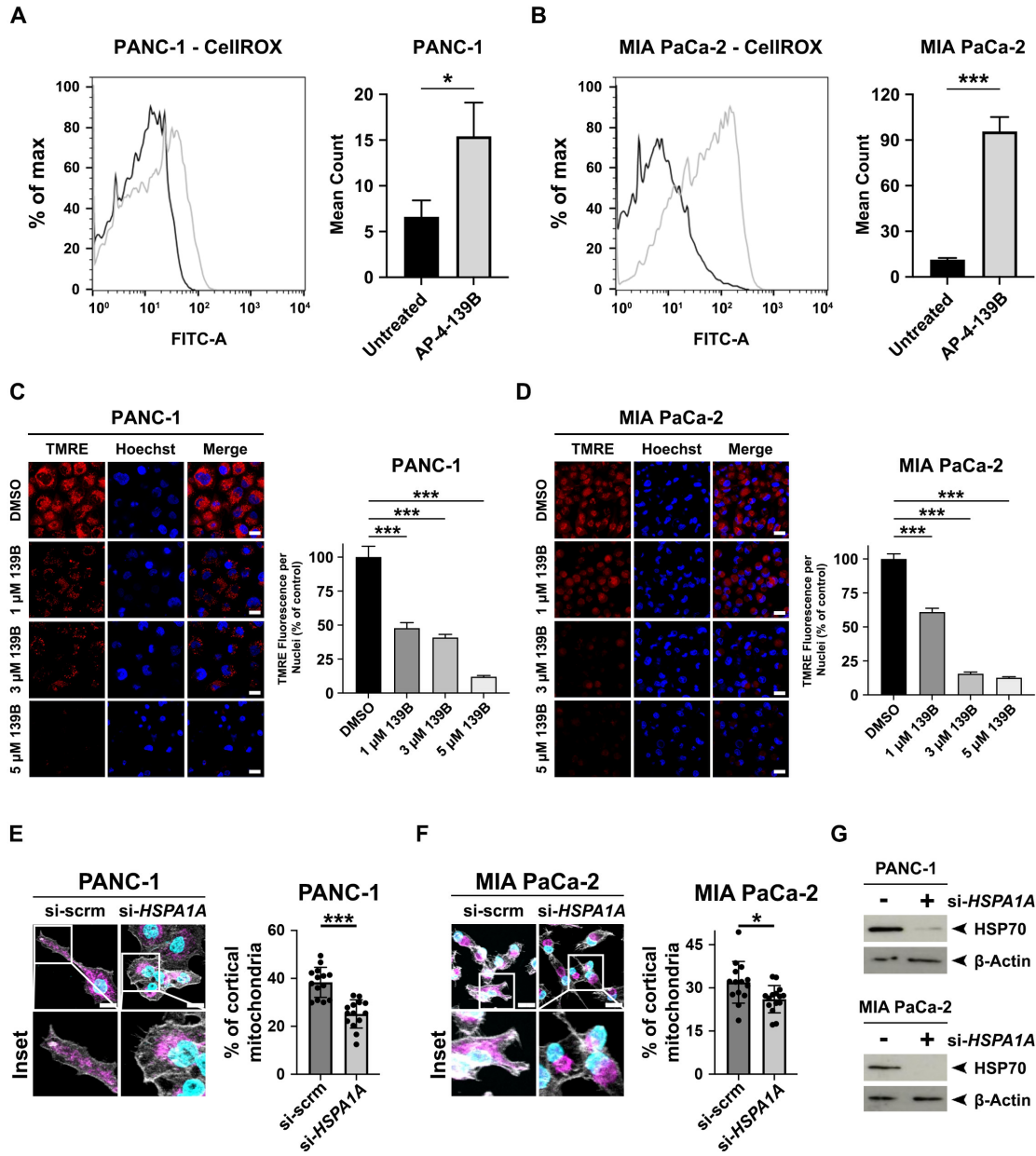
315

316

317

318

Supplemental Figure 1



320
321
322

323 **Supplemental Figure 1. Suppression of HSP70 impairs mitochondrial function and alters**
324 **mitochondrial subcellular localization in PDAC cells.**

325 **A-B.** PANC1 (A) and MIA PaCa-2 (B) cells were treated with 5 μ M of AP-4-139B for 48 hours. Cells
326 were then incubated with CellROX-Green, harvested, and analyzed by flow cytometry to determine ROS
327 production. Fluorescence mean was analyzed and plotted on a histogram. To the right of each histogram
328 is the quantification of mean PANC1 (A) and MIA PaCa-2 (B) CellROX counts in untreated and AP-4-
329 139B treated cells. * p <0.05, *** p <0.001; n =3 independent experiments.

330 **C-D.** PANC-1 and MIA PaCa-2 cells were treated with the indicated doses of AP-4-139B for 24 hours and
331 were stained with TMRE for 20 minutes prior to imaging using a confocal microscope. Hoechst was used
332 to stain nuclei. n =2 independent experiments. For each experiment, six random images were taken and
333 quantified per experimental group. *** p <0.001; bar scale: 20 μ m.

334 **E-F.** PANC-1 and MIA PaCa-2 cells were transfected with a pool of *HSPA1A* siRNA for 48 hours and the
335 percentage of cortical mitochondria were analyzed. Shown are representative images of mitochondria were
336 labeled with 100 nM MitoTracker deep red FM dye (magenta), while actin filaments were stained with
337 phalloidin (white) and nuclei stained with Hoechst (cyan). n =2 independent experiments. Six to eight
338 images were taken per experimental group via confocal microscopy at 40X magnification. * p <0.05,
339 *** p <0.001; bar scale: 20 μ m.

340 **G.** Western blot analysis of HSP70 protein levels following transfection of *HSPA1A* siRNA; GAPDH was
341 used as a loading control.

342

343

344

345

346

347

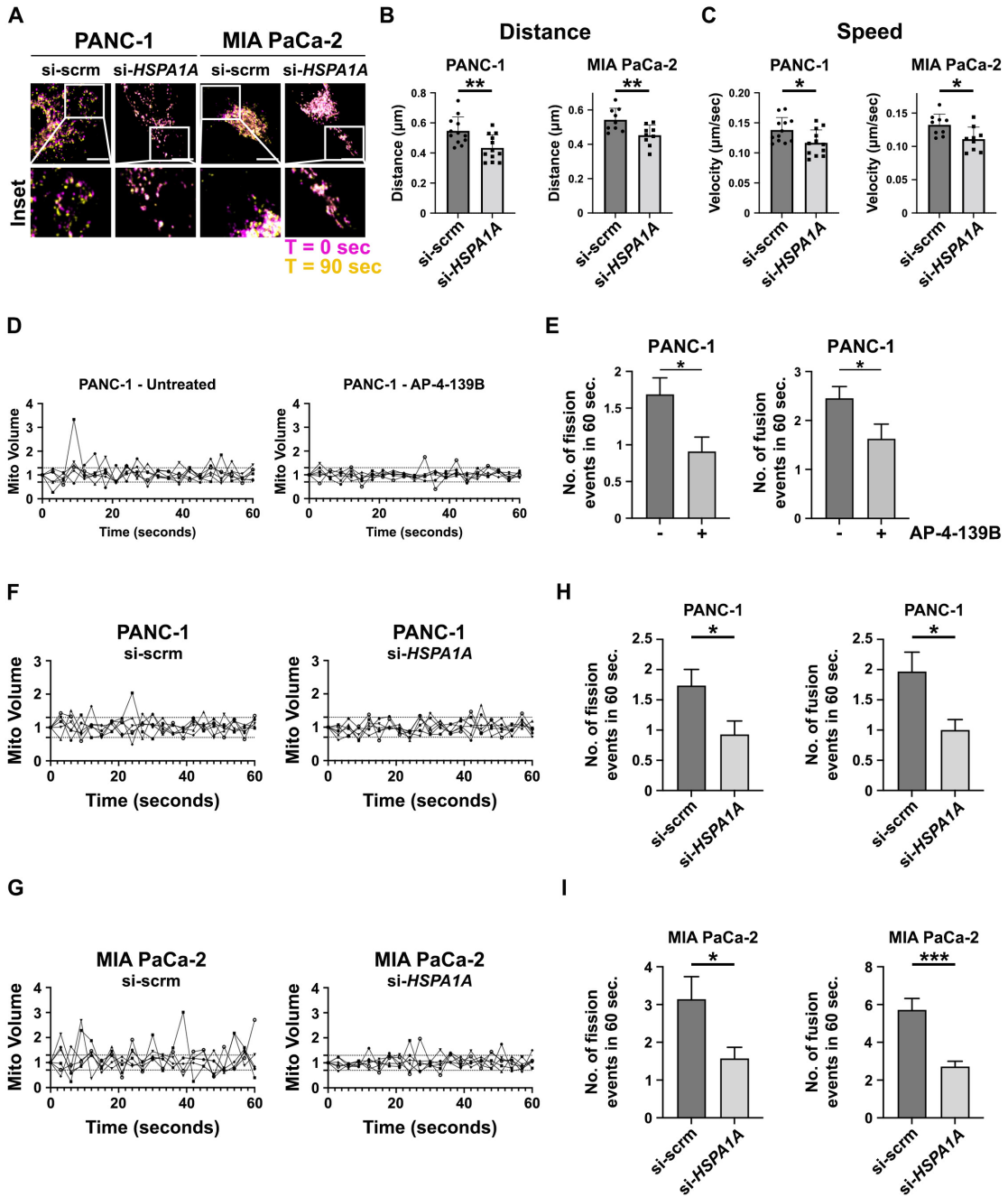
348

349

350

351

Supplemental Figure 2



352
353
354
355

356 **Supplemental Figure 2. Genetic or pharmacological ablation of HSP70 reduces mitochondrial**
357 **motility and impairs mitochondrial dynamics in PDAC cells.**

358 **A.** PANC1 and MIA PaCa-2 cells were transfected with a pool of *HSPA1A* siRNA for 48 hours and were
359 analyzed for mitochondrial motility by time-lapse video-microscopy. Magenta = 0 seconds, yellow = 90
360 seconds, white = overlap; bar scale: 10 μ m.

361 **B-C.** Quantification of (A); mitochondrial motility was measured and the distance (B) and the speed (C)
362 of each mitochondrion were analyzed. 9-12 individual mitochondria were analyzed per treatment group
363 for each cell line. n=2 independent experiments.

364 **D.** PANC-1 cells were treated with 500 nM AP-4-139B for 24hours, followed by staining with MitoTracker
365 Deep Red. Time-lapse video-microscopy was performed by acquiring images every three seconds for 1-
366 minute interval and change in mitochondrial volume over time was measured. n=2 independent biological
367 replicates, with six single cells imaged for each experimental condition.

368 **E.** Quantification of mitochondrial fission (<0.7-fold mitochondrial volume) and fusion (>1.3-fold
369 mitochondrial volume) events in a 1-minute time interval. p<0.05. Data are shown as mean \pm SD.

370 **F-G.** PANC-1 and MIA PaCa-2 cells were transfected with *HSPA1A* siRNA for 48 hours followed by
371 staining with MitoTracker Deep Red. Time-lapse video-microscopy was performed by acquiring images
372 every three seconds for a 1-minute interval and change in mitochondrial volume over time was measured.
373 Line graphs of (F) and (G) are of a single representative experiment; n=three independent biological
374 replicates.

375 **H-I.** Quantification of mitochondrial fission (<0.7-fold mitochondrial volume) and fusion (>1.3-fold
376 mitochondrial volume) events in a 1-minute time interval. Graphs of (G) and (I) are the average of three
377 independent experiments.

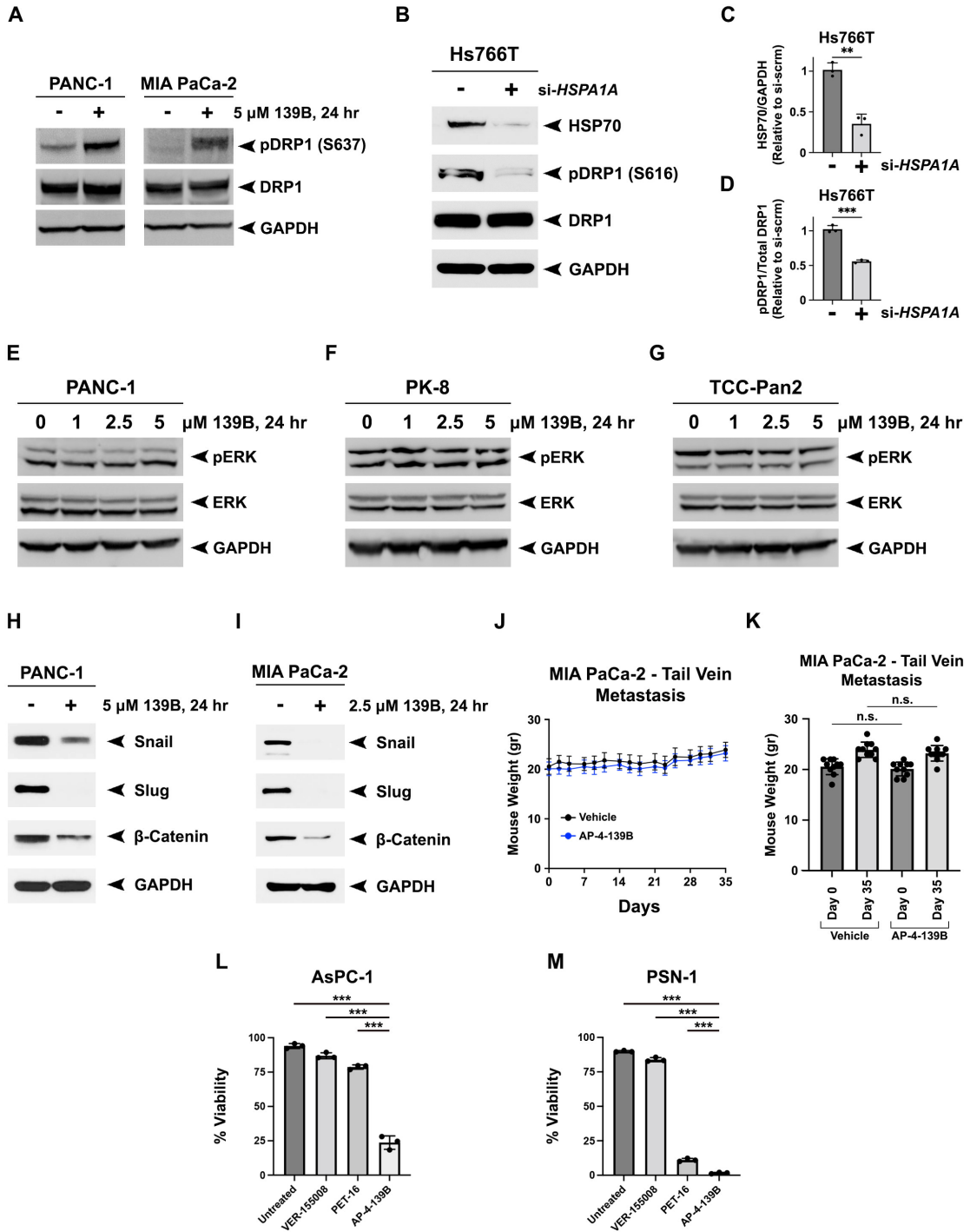
378

379

380

381

Supplemental Figure 3



382

383

384 **Supplemental Figure 3. HSP70 inhibition affects DRP1 phosphorylation in an ERK-independent**
385 **manner and suppresses the metastatic potential of PDAC cells *in vitro* and *in vivo*.**

386 **A.** PANC-1 and MIA PaCa-2 cells were treated with 5 μ M AP-4-139B for 24 hours. Cell lysates were
387 subjected to Western blot analysis and immunoblotted for phospho-DRP1 (S637), total DRP1, and GAPDH
388 (loading control). n=2 independent experiments.

389 **B.** Hs766T cells were transfected with a pool of HSP70 siRNA and were harvested 48 hours later. Cell
390 lysates were subjected to Western blot analysis and immunoblotted for phospho-DRP1 (S616), total DRP1,
391 HSP70 and GAPDH (loading control).

392 **C-D.** Quantification of (B) was performed by obtaining the density of the phospho-DRP1 bands using
393 ImageJ software and normalizing to the level of total DRP1. quantification of HSP70 was normalized to
394 GAPDH. **p<0.01, ***p<0.001. n=three independent experiments.

395 **E-G.** PANC-1, PK-8, and TCC-Pan2 cells were treated with the indicated doses of AP-4-139B for 24 hours.
396 Cell lysates were subjected to Western blot analysis and immunoblotted for phospho-ERK, total ERK, and
397 GAPDH (loading control). n=2 independent experiments.

398 **H-I.** PANC1 (H) and MIA PaCa-2 (I) cells were treated with DMSO (control) or 5 μ M AP-4-139B (or
399 “139B”) for 24 hours. Lysates were extracted and analyzed by Western blot analysis for protein levels of
400 Snail, Slug, β -Catenin, and GAPDH (loading control). n=2 biological replicates.

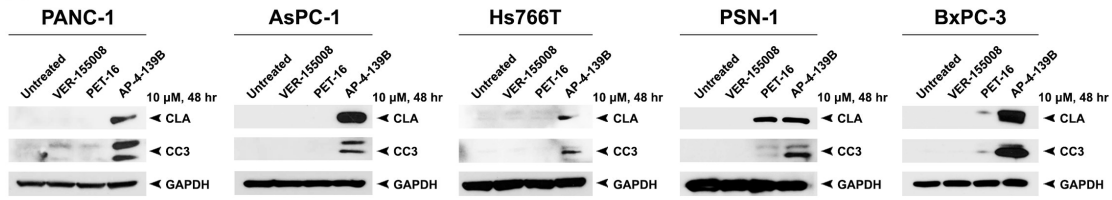
401 **J.** Body weights of mice injected with MIA PaCa-2 cells for tail vein mediated lung metastasis. Weights
402 were measured from the start of the treatment to determine mouse toxicity. n=8 mice per group.

403 **K.** Quantification of (J) at endpoint. Changes in total mouse weight between Day 0 and Day 35 in vehicle
404 and AP-4-139B treatment groups are shown. Data is shown as the mouse weight \pm the standard deviation;
405 n.s., not significant.

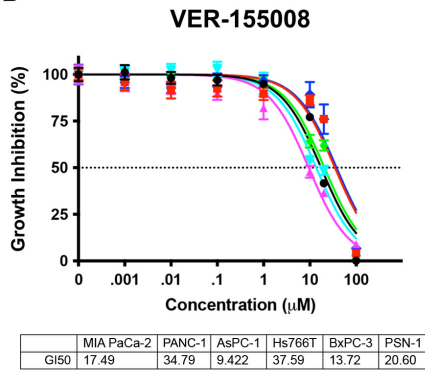
406 **L-M.** AsPC-1 and PSN-1 cells were treated with 10 μ M of VER-155008, PET-16, or AP-4-139B for 48
407 hours. Cells were then subjected to viability assays using trypan blue exclusion. ***p<0.001. n=3
408 independent experiments.

Supplemental Figure 4

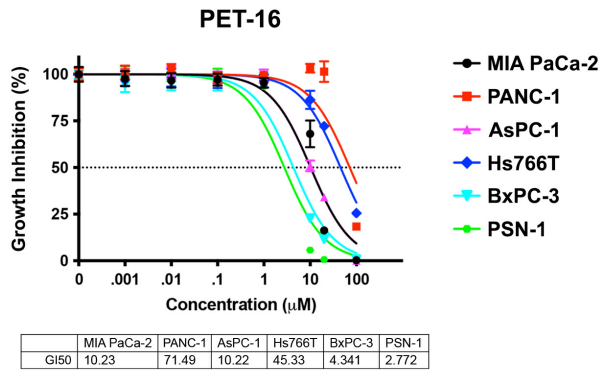
A



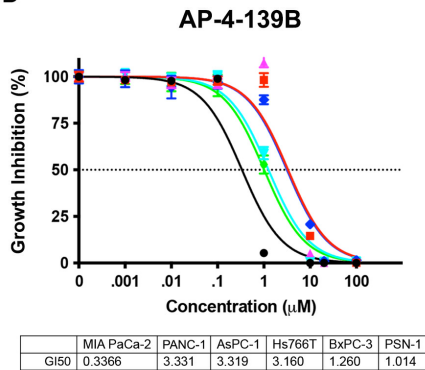
B



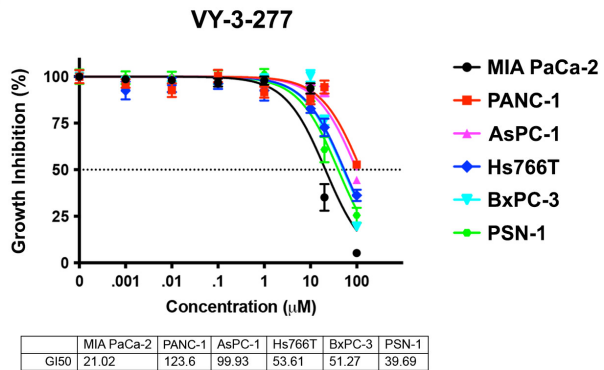
C



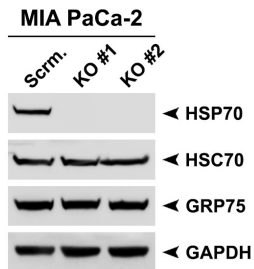
D



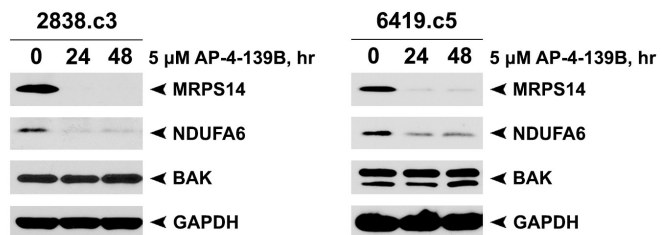
E



F



G



409

410

411 **Supplemental Figure 4. AP-4-139B is a superior HSP70 inhibitor that leads to a reduction of HSP70**
412 **client proteins and induces cell death in PDAC cells.**

413 **A.** Five human PDAC cell lines (PANC1, AsPC-1, Hs766T, PSN-1, and BxPC-3) were plates in 10 cm
414 dishes at a concentration of 5×10^5 cells per plate. The next day, cells were treated with 10 μ M of the
415 indicated inhibitors for 48 hours. Cell lysates were then subjected to Western blot analysis, and
416 immunoblotted for Cleaved Lamin A (CLA), Cleaved Caspase 3 (CC3), and GAPDH (loading control).

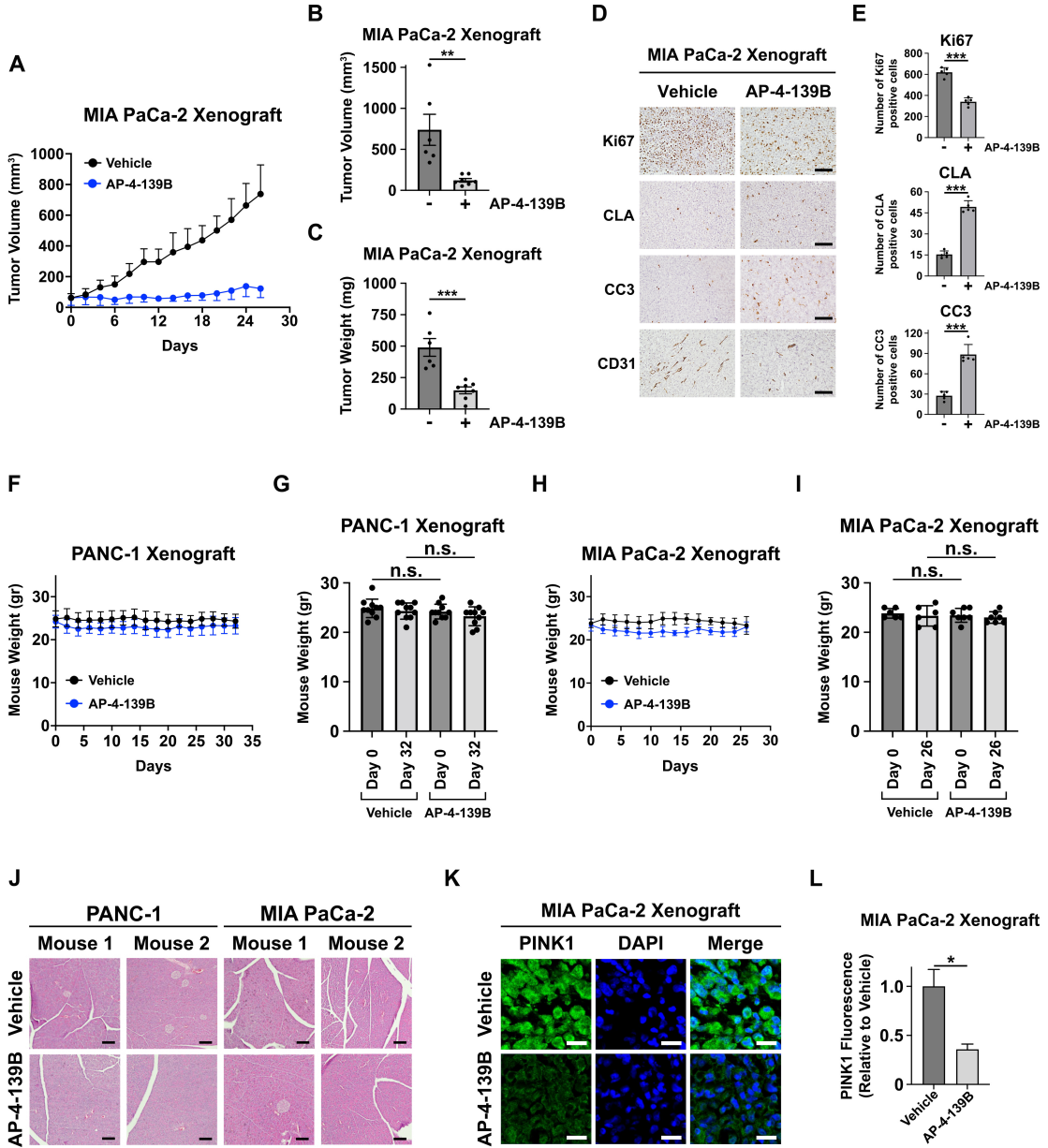
417 **B-E.** A panel of six human PDAC cell lines (MIA PaCa-2, PANC1, AsPC-1, Hs766T, BxPC-3, and PSN-
418 1) were treated with the indicated inhibitors for 72 hours and subjected to Alamar Blue assays. GI_{50} values
419 are from six technical replicates and two biological replicates.

420 **F.** HSP70 knockout (KO) was confirmed by Western blot analysis. Cell lysates from two independent KO
421 clones and a control (sg-scrambled) pool were subjected to Western blot analysis and immunoblotted for
422 HSP70, HSC70, and GRP75, and GAPDH (loading control).

423 **G.** Mouse PDAC cell lines (2838c.3 and 6419c.5) were treated with 5 μ M of AP-4-139B and harvested at
424 the indicated timepoints. Cell lysates were processed for Western blot analysis and immunoblotted for
425 MRPS14, NDUFA6, BAK, and GAPDH (loading control).

426
427
428
429
430
431
432
433
434
435
436
437
438
439
440
441
442
443

Supplemental Figure 5



444
445
446
447

448 **Supplemental Figure 5. HSP70 inhibition limits PDAC tumor progression *in vivo*.**

449 **A.** 2.5×10^6 MIA PaCa-2 cells were injected subcutaneously into the right flanks of 8–10-week-old female
450 NSG mice. Once tumors reached an approximate size of 75 mm^3 , mice were randomly sorted into vehicle
451 and AP-4-139B treated groups. AP-4-139B was treated at a dose of 10mg/kg every other day, and tumors
452 were measured every other day using a digital caliper. $n=6-7$ mice per group.

453 **B-C.** Quantification of tumor volume (B) and tumor weight (C) at endpoint; ** $p < 0.01$, *** $p < 0.001$.

454 **D.** IHC analysis of MIA PaCa-2 xenograft tumors treated with AP-4-139B. Shown are representative
455 images (five random fields of view per condition) of Ki67, Cleaved Lamin A, Cleaved Caspase 3, and
456 CD31. $n=5$ mice per group; scale bar: 100 μm .

457 **E.** Quantification of (D); *** $p < 0.001$.

458 **F-I.** Body weights of mice injected with PANC1 (F-G) and MIA PaCa-2 (H-I) tumor xenografts. Weights
459 were measured at the start of the treatment to determine mouse toxicity. (G, I) Quantification of change in
460 total mouse weight from F and H. n.s. not significant, $n=6-10$ mice per group.

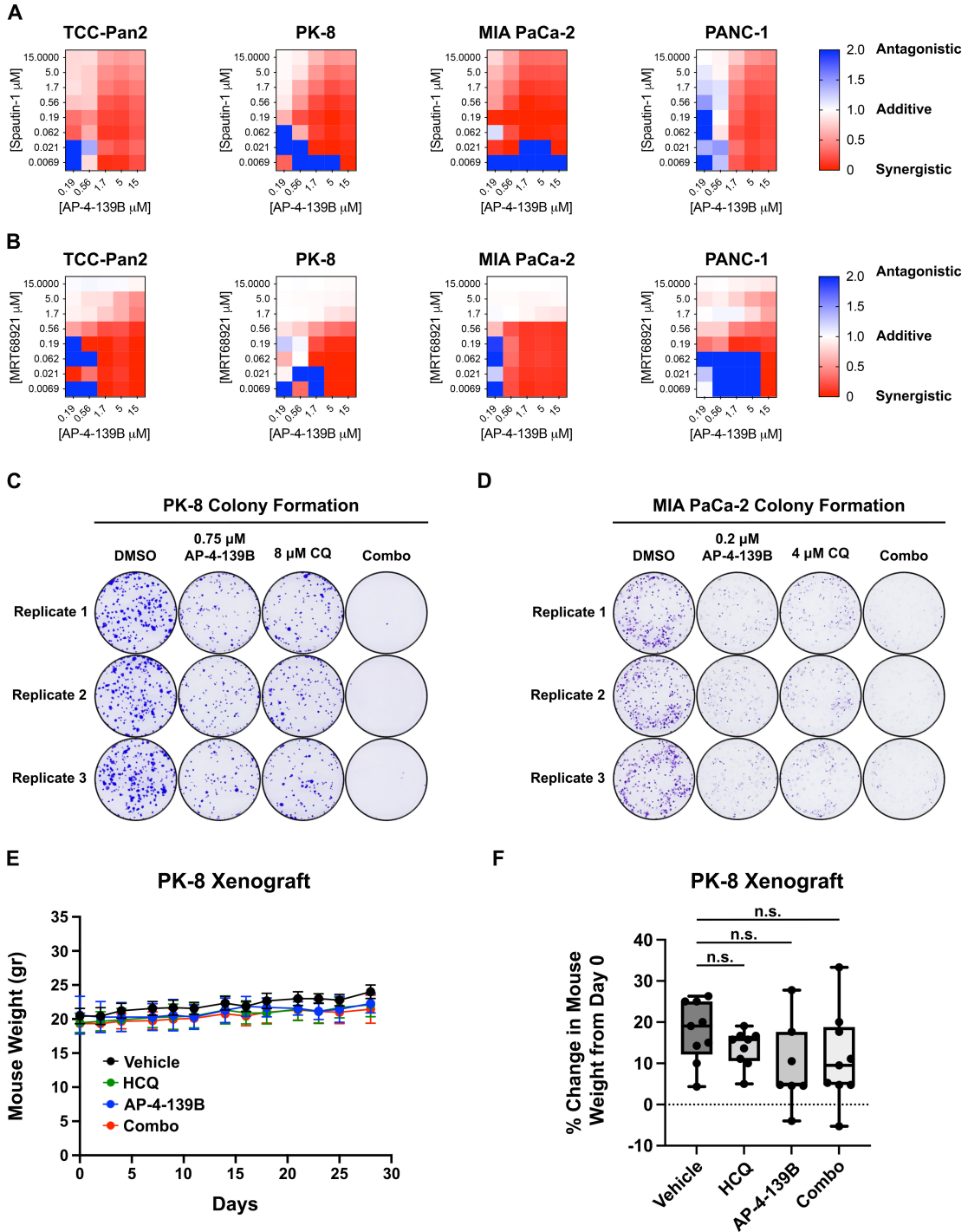
461 **J.** H&E staining of pancreas tissues of mice injected with PANC1 or MIA PaCa-2 xenografts. Tissues
462 were collected at the end of the study. Bar scale: 100 μm .

463 **K.** Immunofluorescence (IF) analysis of PINK1 (green) was performed on MIA PaCa-2 xenograft tumors,
464 and counterstained with DAPI (blue). Bar scale: 20 μm .

465 **L.** Quantification of (K); $n=3$ mice per group. * $p < 0.05$.

466
467
468
469
470
471
472
473
474
475

Supplemental Figure 6



476

477

478 **Supplemental Figure 6. AP-4-139B synergizes with autophagy inhibition in human PDAC cell lines**
479 **and in a xenograft model.**

480 **A-B.** TCC-Pan2, PK-8, MIA PaCa-2, and PANC-1 cells were treated for 72 hours with HSP70i (AP-4-
481 139) in combination with one of the following autophagy inhibitors, Spautin-1 or MRT68921, at the
482 indicated concentrations. Cells were stained for viability with Calcein and imaged using a Celigo image
483 cytometer. Cell numbers at endpoint were normalized to vehicle-treated control (100% growth) for each
484 cell line. Heatmaps representing BLISS independence scores corresponding using proliferation indices for
485 each condition. Scores <1 indicate synergy (red), score =1 indicated additivity (white), and scores >1
486 indicate antagonism (blue). n=3 independent experiments.

487 **C-D.** PK-8 and MIA PaCa-2 cells were seeded in 60-mm dishes at a concentration of 500 cells per dish
488 and were subjected to colony formation assays in the presence of the indicated compounds: AP-4-139B,
489 CQ, or the combination of both compounds (Combo). Cells were fixed and stained with 0.5% Crystal
490 Violet after seven (MIA PaCa-2) or fourteen (PK-8) days. Shown are images of all three replicates of a
491 single experiment; one replicate for each condition per cell line shown was used to generate Figure 7C-D.
492 All colony formation assays were repeated three times.

493 **E.** Relative mouse weights throughout the course of the PK-8 xenograft mouse study described in Figure
494 7E-F. Mouse weights were measured three times per week for the entire 28-day course of treatment. n=7-
495 9 mice per group.

496 **F.** Quantification of percent change in PK-8 xenograft mouse weights assessed over 28 days treated with
497 the following: 1. Vehicle (control), 2. Hydroxychloroquine (50 mg/kg daily), 3. AP-4-139B (10 mg/kg every
498 other day), or 4. the combination of both agents at the doses indicated. n.s. not significant.

499
500
501
502
503
504
505

506 **Supplementary References**

507

- 508 1 Barnoud, T., Parris, J. L. D. & Murphy, M. E. Tumor cells containing the African-Centric
509 S47 variant of TP53 show increased Warburg metabolism. *Oncotarget* **10**, 1217-1223,
510 doi:10.18632/oncotarget.26660 (2019).
- 511 2 Basu, S., Barnoud, T., Kung, C. P., Reiss, M. & Murphy, M. E. The African-specific S47
512 polymorphism of p53 alters chemosensitivity. *Cell Cycle* **15**, 2557-2560,
513 doi:10.1080/15384101.2016.1215390 (2016).
- 514 3 Barnoud, T., Donninger, H. & Clark, G. J. Ras Regulates Rb via NORE1A. *J Biol Chem*
515 **291**, 3114-3123, doi:10.1074/jbc.M115.697557 (2016).
- 516 4 Donninger, H., Barnoud, T., Nelson, N., Kassler, S., Clark, J., Cummins, T. D. *et al.*
517 RASSF1A and the rs2073498 Cancer Associated SNP. *Front Oncol* **1**, 54,
518 doi:10.3389/fonc.2011.00054 (2011).
- 519 5 Barnoud, T., Budina-Kolomets, A., Basu, S., Leu, J. I., Good, M., Kung, C. P. *et al.*
520 Tailoring Chemotherapy for the African-Centric S47 Variant of TP53. *Cancer Res* **78**,
521 5694-5705, doi:10.1158/0008-5472.CAN-18-1327 (2018).
- 522 6 Parris, J. L. D., Barnoud, T., Leu, J. I., Leung, J. C., Ma, W., Kirven, N. A. *et al.* HSP70
523 inhibition blocks adaptive resistance and synergizes with MEK inhibition for the treatment
524 of NRAS-mutant melanoma. *Cancer Res Commun* **1**, 17-29, doi:10.1158/2767-9764.crc-
525 21-0033 (2021).
- 526 7 Diehl, J. N., Klomp, J. E., Snare, K. R., Hibshman, P. S., Blake, D. R., Kaiser, Z. D. *et al.*
527 The KRAS-regulated kinome identifies WEE1 and ERK coinhibition as a potential
528 therapeutic strategy in KRAS-mutant pancreatic cancer. *J Biol Chem* **297**, 101335,
529 doi:10.1016/j.jbc.2021.101335 (2021).
- 530 8 Fouquier, J. & Guedj, M. Analysis of drug combinations: current methodological
531 landscape. *Pharmacol Res Perspect* **3**, e00149, doi:10.1002/prp2.149 (2015).
- 532 9 Bryant, K. L., Stalnecker, C. A., Zeitouni, D., Klomp, J. E., Peng, S., Tikunov, A. P. *et al.*
533 Combination of ERK and autophagy inhibition as a treatment approach for pancreatic
534 cancer. *Nat Med* **25**, 628-640, doi:10.1038/s41591-019-0368-8 (2019).
- 535 10 Hobbs, G. A., Baker, N. M., Miermont, A. M., Thurman, R. D., Pierobon, M., Tran, T. H.
536 *et al.* Atypical KRAS(G12R) Mutant Is Impaired in PI3K Signaling and Macropinocytosis
537 in Pancreatic Cancer. *Cancer Discov* **10**, 104-123, doi:10.1158/2159-8290.CD-19-1006
538 (2020).
- 539 11 Basu, S., Gnanapradeepan, K., Barnoud, T., Kung, C. P., Tavecchio, M., Scott, J. *et al.*
540 Mutant p53 controls tumor metabolism and metastasis by regulating PGC-1alpha. *Genes*
541 *Dev* **32**, 230-243, doi:10.1101/gad.309062.117 (2018).
- 542 12 Gnanapradeepan, K., Leu, J. I., Basu, S., Barnoud, T., Good, M., Lee, J. V. *et al.* Increased
543 mTOR activity and metabolic efficiency in mouse and human cells containing the African-
544 centric tumor-predisposing p53 variant Pro47Ser. *Elife* **9**, doi:10.7554/eLife.55994 (2020).
- 545 13 Bertolini, I., Ghosh, J. C., Kossenkov, A. V., Mulugu, S., Krishn, S. R., Vaira, V. *et al.* Small
546 Extracellular Vesicle Regulation of Mitochondrial Dynamics Reprograms a Hypoxic
547 Tumor Microenvironment. *Dev Cell* **55**, 163-177 e166, doi:10.1016/j.devcel.2020.07.014
548 (2020).
- 549 14 Bertolini, I., Keeney, F. & Altieri, D. C. Protocol for assessing real-time changes in
550 mitochondrial morphology, fission and fusion events in live cells using confocal
551 microscopy. *STAR Protoc* **2**, 100767, doi:10.1016/j.xpro.2021.100767 (2021).

- 552 15 Budina-Kolomets, A., Webster, M. R., Leu, J. I., Jennis, M., Krepler, C., Guerrini, A. *et al.*
553 HSP70 Inhibition Limits FAK-Dependent Invasion and Enhances the Response to
554 Melanoma Treatment with BRAF Inhibitors. *Cancer Res* **76**, 2720-2730,
555 doi:10.1158/0008-5472.CAN-15-2137 (2016).
- 556 16 Bertolini, I., Perego, M., Ghosh, J. C., Kossenkov, A. V. & Altieri, D. C. NFkappaB
557 activation by hypoxic small extracellular vesicles drives oncogenic reprogramming in a
558 breast cancer microenvironment. *Oncogene* **41**, 2520-2525, doi:10.1038/s41388-022-
559 02280-3 (2022).
- 560 17 Akbulut, O., Lengerli, D., Saatci, O., Duman, E., Seker, U. O. S., Isik, A. *et al.* A Highly
561 Potent TACC3 Inhibitor as a Novel Anticancer Drug Candidate. *Mol Cancer Ther* **19**,
562 1243-1254, doi:10.1158/1535-7163.MCT-19-0957 (2020).
- 563 18 Assidicky, R., Tokat, U. M., Tarman, I. O., Saatci, O., Ersan, P. G., Raza, U. *et al.* Targeting
564 HIF1-alpha/miR-326/ITGA5 axis potentiates chemotherapy response in triple-negative
565 breast cancer. *Breast Cancer Res Treat* **193**, 331-348, doi:10.1007/s10549-022-06569-5
566 (2022).
- 567 19 Saatci, O., Kaymak, A., Raza, U., Ersan, P. G., Akbulut, O., Banister, C. E. *et al.* Targeting
568 lysyl oxidase (LOX) overcomes chemotherapy resistance in triple negative breast cancer.
569 *Nat Commun* **11**, 2416, doi:10.1038/s41467-020-16199-4 (2020).
- 570 20 Goldman, M. J., Craft, B., Hastie, M., Repecka, K., McDade, F., Kamath, A. *et al.*
571 Visualizing and interpreting cancer genomics data via the Xena platform. *Nat Biotechnol*
572 **38**, 675-678, doi:10.1038/s41587-020-0546-8 (2020).
- 573 21 Moffitt, R. A., Marayati, R., Flate, E. L., Volmar, K. E., Loeza, S. G., Hoadley, K. A. *et al.*
574 Virtual microdissection identifies distinct tumor- and stroma-specific subtypes of
575 pancreatic ductal adenocarcinoma. *Nat Genet* **47**, 1168-1178, doi:10.1038/ng.3398 (2015).
- 576 22 Barnoud, T., Leung, J. C., Leu, J. I., Basu, S., Poli, A. N. R., Parris, J. L. D. *et al.* A Novel
577 Inhibitor of HSP70 Induces Mitochondrial Toxicity and Immune Cell Recruitment in
578 Tumors. *Cancer Res* **80**, 5270-5281, doi:10.1158/0008-5472.CAN-20-0397 (2020).
579